Static recrystallization kinetics in warm worked vanadium microalloyed steels

C. García-Mateo, B. López, J.M. Rodriguez-Ibabe *

CEIT and ESII, Materials Department, University of Navarra, P° M. Lardizabal 15, 20018 San Sebastián, Basque Country, Spain

Abstract

The effect of vanadium on static recrystallization kinetics of vanadium microalloyed carbon steels after simulating warm working conditions has been determined using the stress relaxation method in plane strain compression tests. In the warm working regime, undissolved fine V(C,N) precipitates promote a fine austenite grain size during reheating and interact with the recrystallization process after working, leading to longer recrystallization times in comparison with plain C–Mn steels. The interaction between precipitates and recrystallization is different to that observed for hot working conditions, retarding the total recrystallization process and thus resulting in a lower value of the Avrami exponent and a longer $t_{0.5}$ time. © 2001 Elsevier Science B.V. All rights reserved.

Keywords: Warm working; Static Recrystallization; V Microaddition

1. Introduction

Near-net-shape forming technologies are becoming one of the main procedures to obtain more competitive final products. Warm forging route belongs to these technologies, presenting different advantages in comparison with conventional hot and cold forging. By warm forging, it is possible to produce parts close to their final shape and, simultaneously, to reduce or eliminate cold working. In conventional hot forging, microalloying with Ti or Ti–V has become a main procedure to obtain ferritic–pearlitic steels with good strength–toughness combinations [1,2]. These properties are achieved by an adequate austenite grain size control due to fine TiN particles and by a precipitation strengthening of very fine V(C,N) particles during cooling. In the case of warm working, the low soaking temperatures applied (usually under 900°C) lead to fine austenitic microstructures and, in consequence, the microaddition of Ti is not required. On the other hand, since the low reheating temperature does not allow the complete dissolution of V(C,N) precipitates, not all of

the vanadium will contribute to the final strength of the steel via precipitation hardening, limiting its possible application as a microalloying element. Nevertheless, if an appropriate V(C,N) precipitation is obtained in the as-rolled product, vanadium can play different roles during warm forging processes, which can lead to a significant improvement in the final mechanical behavior. Depending on the reheating temperature, which will define the amount of undissolved precipitates, vanadium microalloying can control austenite grain growth during reheating, delay the static recrystallization of austenite and induce precipitation strengthening [3,4]. Among these possible different effects assigned to vanadium, the purpose of the present study is to focus on the effects that undissolved V(C,N) particles can have on the austenite static recrystallization kinetics during warm working conditions.

Static recrystallization kinetics in C–Mn and microalloyed steels have been investigated extensively, and several regression equations have been proposed. The influence of prior austenite grain size (D_o), applied equivalent strain (ε), deformation temperature (T) and strain rate ($\dot{\varepsilon}$) on the kinetics of static recrystallization are conveniently expressed in terms of the time required to induce some specified recrystallization fraction, say

---

* Corresponding author. Tel.: +34-9432-12800; fax: +34-9432-13076.

E-mail address: jmribabe@ceit.es (J.M. Rodriguez-Ibabe).

$X = 0.5$. The expression that takes into account the influence of the different parameters that intervene on the value of $t_{0.5}$ is:

$$t_{0.5} = A\varepsilon^{-p}\dot{\varepsilon}^{-q}D_o^m \exp(Q/RT) \qquad (1)$$

where m, p and q are constants, ε the applied strain, $\dot{\varepsilon}$ the strain rate, D_o the initial austenite grain size and Q is the activation energy for static recrystallization.

The driving force for static recrystallization can be taken to be the difference in dislocation density between the deformed or recovered matrix and the recrystallized matrix. On the other hand, the pinning forces caused by particles and by solutes are responsible for the retardation of recrystallization and can notably increase the value of $t_{0.5}$ [5–7]. In conventional hot working of microalloyed steels, strain-induced precipitation is the main procedure to obtain the suppression or retardation of recrystallization. In this case, after soaking, the microalloying element is in solution and, during the deformation at lower temperatures, the austenite is supersaturated with respect to the element, promoting its precipitation. In contrast, in the case of warm working of V microalloyed steels, those particles, which have not been dissolved during a previous reheating treatment, will also act in the steel both during deformation and recrystallization, and in combination with the remaining vanadium in solution.

The main objective of this work is to study the effects of the application of warm working on the austenite static recrystallization process in vanadium microalloyed steels, considering a range of temperatures to obtain different precipitate volume fractions that remain undissolved in the austenite prior to deformation.

2. Material and experimental procedure

Three steels, whose chemical compositions are listed in Table 1, were used in the present work. V1 and V2 are vanadium microalloyed steels with different C and V contents, and the third steel is a conventional C–Mn forging steel with higher C and lower Mn contents. Warm working was simulated by plane strain compression tests. All the tests were carried out at a constant temperature and at a strain rate of 10 s^{-1}. Specimens $(25 \times 50 \times 10 \text{ mm}^3)$ machined from the as-received industrially hot rolled bars were heated in a resistance

furnace and soaked at the specified temperature for 10 min before testing. The tests were performed inside the furnace, using tool faces lubricated with boron nitride in order to reduce frictional effects. After deformation, the static recrystallization kinetics were analyzed by the stress relaxation method [8,9]. Once the deformation was applied, the ram displacement was kept constant and the load change monitored as a function of time. Prior to the tests, the machine and tools stiffness was determined for each testing temperature, and the relaxation curves corrected by the corresponding values, with the objective of separating possible machine effects from microstructural events taking place in the specimen. During each relaxation test, the data acquisition frequency has been modified using different frequencies at the different test stages in order to obtain an adequate distribution of data against time.

For most temperatures and steels, the applied deformation was $\varepsilon = 0.3$; for some specific conditions, the samples were deformed to a nominal strain value of $\varepsilon \approx 0.4$. Different test temperatures, 800, 835, 870 and 1025°C, were selected and controlled by a thermocouple inserted into the center of the specimen. From the tests, the load–displacement curves were obtained and, after correcting for lateral spread of the specimen and for the frictional effects [10], the true stress–strain curves were determined.

Initial austenite grain size was determined from samples quenched after the soaking treatment. The microstructure was revealed using an aqueous picric acid etchant with a wetting reagent. Measurements were performed using a quantitative image analyzer. To study the distribution of V(C,N) particles, carbon extraction replicas were prepared and examined in a Philips CM12 STEM. The precipitates were studied in both vanadium microalloyed steels in the as-received condition and in quenched samples after reheating to 835 and 870°C. For quantification purposes, between 600 and 900 particle diameters were measured from each specimen.

3. Results

The influence of the reheating temperature prior to deformation on the austenite grain size is shown in Fig. 1. In both V microalloyed steels, a very fine austenite

Table 1
Chemical composition of the steels (wt.%)

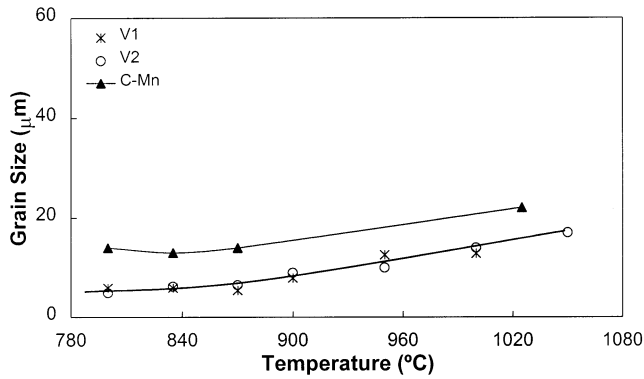| Steel	C	Mn	Si	P	S	V	Al	N
V1	0.24	1.56	0.28	0.022	0.003	0.18	0.019	0.0099
V2	0.33	1.49	0.25	0.015	0.002	0.24	0.027	0.0100
C–Mn	0.47	0.78	0.24	0.007	0.032	–	0.025	0.0090

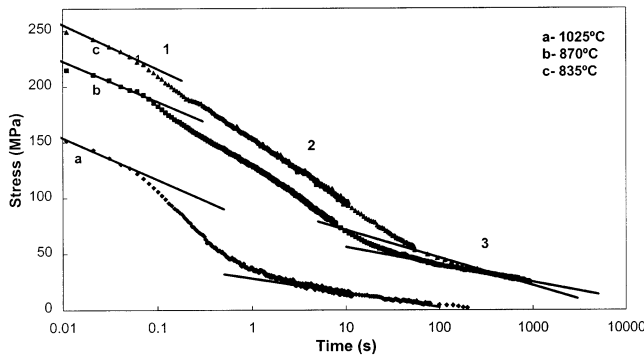Fig. 1. Influence of the reheating temperature on the initial austenite grain size.

Fig. 2. Stress versus log(time) curves obtained from relaxation tests ($\varepsilon = 0.3$, $\dot{\varepsilon} = 10 \ s^{-1}$) for steel V1.
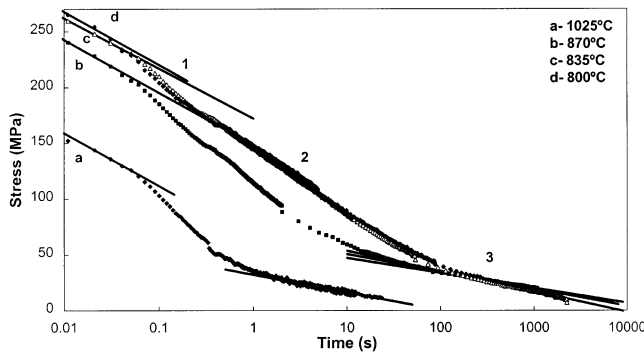

Fig. 3. Stress versus log(time) curves obtained from relaxation tests ($\varepsilon = 0.3$, $\dot{\varepsilon} = 10 \ s^{-1}$) for steel V2.

grain size was obtained, with a mean value close to 5–6 μm in the range 800–870°C. For the same temperature interval, the C–Mn steel exhibits a grain size of 14 μm. From Fig. 1, it can be seen that, in all the steels, the heat treatment at 1025°C promotes a slight grain growth. Finally, both V microalloyed steels show the same trend in the analyzed temperature range.

Figs. 2–4 show the stress relaxation curves obtained for the three steels at different testing temperatures, for the tests performed after an applied deformation of $\varepsilon = 0.3$. In the stress–log(time) curves, three regions can

be distinguished. In the first part of the curves, the stress level decreases at a constant rate (first linear portion); the second part shows a much more rapid decrease; and, finally, in the third, the relaxation is again constant but with a lower rate (second linear portion). The stress decrement in the first linear part of the curve is related to the recovery of the hardened austenite, while in the second part the occurrence of static recrystallization promotes more rapid softening with a change in the slope of the curve. Finally, when recrystallization has been completed, a further decrease in the slope takes place due to the stress relaxation of the soft recrystallized austenite. As can be observed in the curves, the decrease in the testing temperature leads to higher stress values and, simultaneously, shifts the end of the recrystallization region towards longer times.

As is shown in Figs. 2–4, the evolution of stress with time in regions 1 and 3 of the curves can be described by simple straight lines of the form [8,9]:

$$\sigma = \sigma_o - \alpha \log t \qquad (2)$$

where σ and t are the true stress and the relaxation time, respectively, and σ_o and α are constants. The corresponding values of α and σ_o obtained for each region (1 and 3) at the different test conditions are shown in Table 2. In the second region, it is simply assumed that the partially recrystallized material is formed by two compounds, one being the work hardened material (region 1) and the other the fully softened microstructure (region 3). The stress level in this region can be expressed by applying the law of mixtures and taking into account the relative fractions of each compound present at a given time as follows [9]:

$$\sigma = (1 - X)(\sigma_{o1} - \alpha_1 \log t) + X(\sigma_{o3} - \alpha_3 \log t) \qquad (3)$$

where X represents the recrystallized fraction, and the subscripts 1 and 3 refer to the first (work hardened material) and the third (soft recrystallized material) regions of the relaxation curve, respectively. From Eq. (3), the recrystallized fraction at a given time can be calculated.
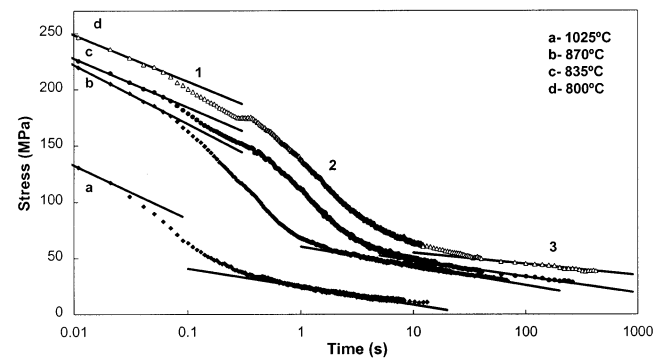

Fig. 4. Stress versus log(time) curves obtained from relaxation tests ($\varepsilon = 0.3$, $\dot{\varepsilon} = 10 \ s^{-1}$) for C–Mn steel.

Table 2
Constants σ_o and α calculated from the stress relaxation rate equation (Eq. (2)), and parameters n and $t_{0.5}$ of the Avrami equation

Steel	Temperature (°C)	ε	α_1 (MPa)	σ_{o1} (MPa)	α_3 (MPa)	σ_{o3} (MPa)	n	$t_{0.5}$ (s)
V1	1025	0.3	37.52	79.1	12.72	28.1	1.1	0.3
	1025	0.4	39.92	79.7	17.81	39.3	0.9	0.2
	870	0.3	36.09	150.5	15.69	72.1	0.6	3.6
	835	0.3	39.79	176.1	24.83	96.6	0.5	5.2
	835	0.4	42.25	187.7	21.55	93.8	0.5	3.6
V2	1025	0.3	47.44	64.1	15.96	32.2	1.1	0.3
	870	0.3	51.83	139.8	13.52	60.8	0.5	2.1
	835	0.3	44.77	172.2	18.38	72.2	0.4	7.1
	800	0.3	47.34	176.9	15.63	66.4	0.4	10.9
C–Mn	1025	0.3	47.41	37.7	16.09	24.6	1.1	0.1
	870	0.3	52.55	116.0	17.22	60.5	1.2	0.4
	835	0.3	43.64	140.4	14.53	62.7	1.1	1.4
	835	0.45	58.33	136.6	14.23	64.5	1.1	0.9
	800	0.3	41.63	165.4	10.07	65.2	0.7	2.2

The evolution of the recrystallized fraction with time, determined by Eq. (3) from the second region of Figs. 2–4, is illustrated in Figs. 5–7 for the different steels and testing temperatures used in the present work. From the figures, it is clearly evident that a decrease in temperature shifts the recrystallization curves to longer times. These curves show the typical sigmoidal shape that can be described by the modified Avrami equation:

$$X = 1 - \exp[-\ln 2(t/t_{0.5})^n] \qquad (4)$$

From Eq. (4), the values of $t_{0.5}$ (time required for 50% recrystallization fraction) and the Avrami exponent n have been calculated. The resulting values are shown in Table 2. As can be observed from this table, the exponent n takes values close to 1 in the case of the plain carbon steel and also at the highest temperature, 1025°C, in both V microalloyed steels. However, under the other conditions, lower n values, ranging between 0.4 and 0.6, have been obtained. In relation to the time $t_{0.5}$, it can be concluded from the data reported in Table 2 that there is a significant dependence of this parameter on temperature. As expected, decreasing the temperature requires longer times for recrystallization to occur. Additionally, it can be observed that the times determined for the plain carbon steel are shorter that those measured in both microalloyed steels.

The V(C,N) particle size distributions in the as-received condition and in quenched samples after heat treatments at 835 and 870°C are shown in Figs. 8 and 9 for V1 and V2 steels, respectively. Fig. 10 shows an example of the precipitation observed in steel V1 in the as-received material and after reheating to 870°C. In the as-received condition, mean particle sizes of 8 and 14 nm have been measured in steels V1 and V2, respectively. However, from Figs. 8 and 9, it is clearly evident that, during the reheating prior to deformation, precipitate coarsening takes place. For steel V1, this effect is small at the reheating temperature of 835°C, giving a

mean value of 11 nm, but becomes more significant at 870°C, resulting in a mean size of 21 nm. For steel V2, precipitate coarsening is also observed but the difference between both reheating temperatures is smaller than for the other steel; 18 nm at 835°C compared with 20 nm measured at 870°C. Considering the particle size distribution, an increase in reheating temperature shifts the histograms towards coarser sizes in both steels.
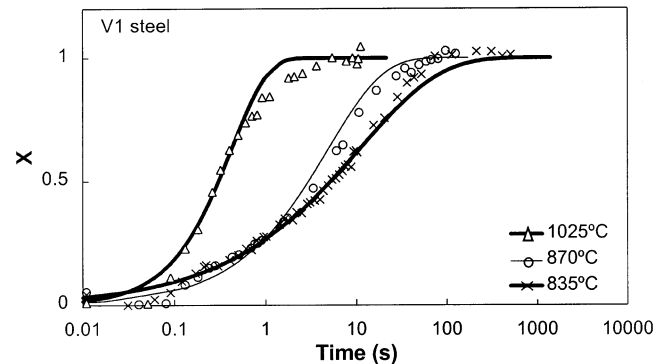
Fig. 5. Softening curves obtained from relaxation tests and corresponding Avrami curves for steel V1.
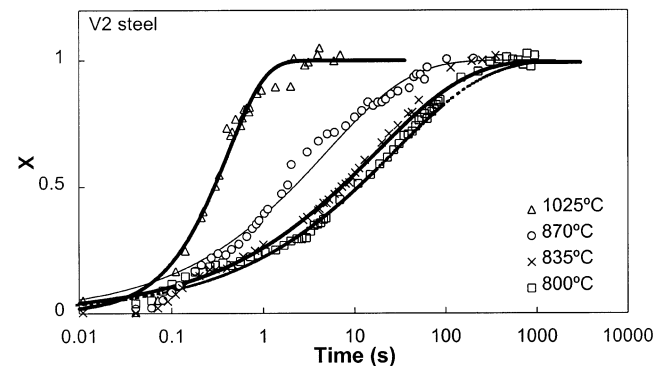
Fig. 6. Softening curves obtained from relaxation tests and corresponding Avrami curves for steel V2.
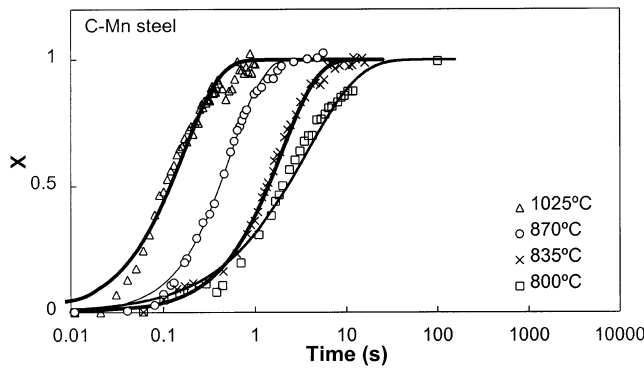
Fig. 7. Softening curves obtained from relaxation tests and corresponding Avrami curves for C–Mn steel.

on austenite grain boundaries in both vanadium microalloyed steels clearly prevents grain growth, leading to very fine austenite grain sizes in the warm working temperature regime. Similarly, in the case of C–Mn steel, the well-known beneficial effect of AlN particles in preventing grain growth is also observed, although less austenite grain refinement is observed in the latter as compared with vanadium microalloyed steels at the same temperature range. These results are in agreement with previous data published by Mazzare et al. [11], where a finer austenite was obtained at 900°C for steels microalloyed with V and V + Nb than for an aluminium-killed steel.

The static recrystallization kinetics of the different materials has been analyzed in terms of the time required to reach a 50% recrystallized fraction ($t_{0.5}$). The general expression for $t_{0.5}$ shown in Eq. (1) includes the
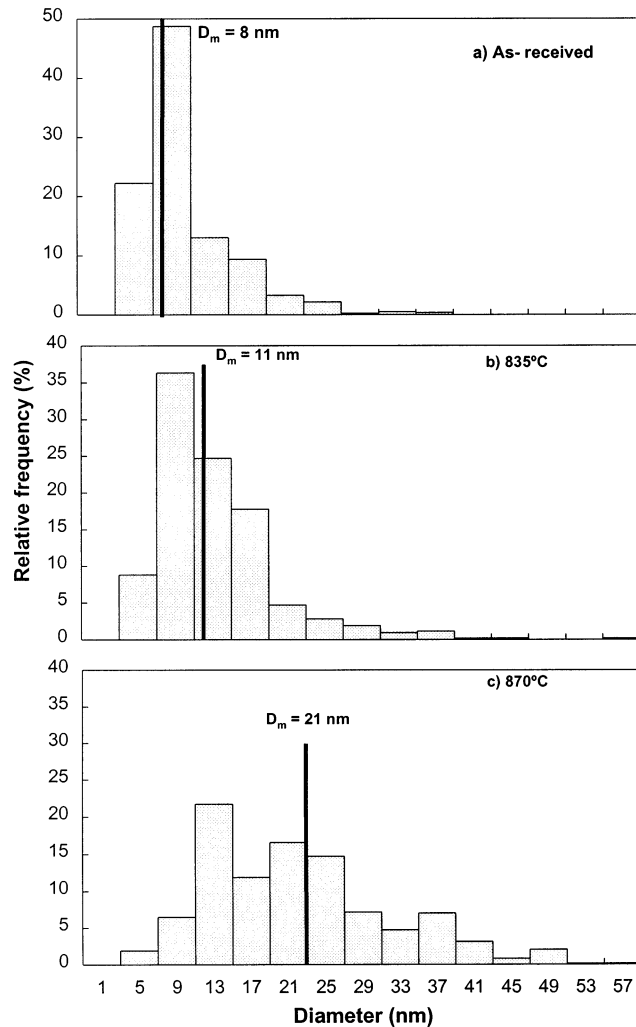

Fig. 8. Evolution of the size distribution of V(C,N) precipitates in steel V1 (a) as-received, (b) after soaking at 835°C and (c) after soaking at 870°C.
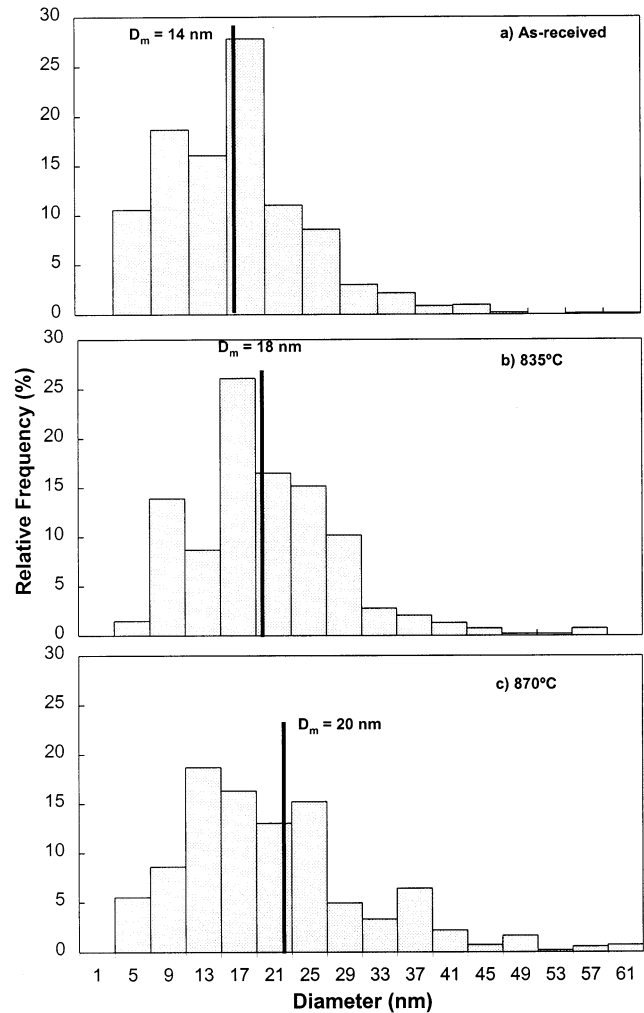

Fig. 9. Evolution of the size distribution of V(C,N) precipitates in steel V2 (a) as-received, (b) after soaking at 835°C and (c) after soaking at 870°C.

4. Discussion

From Fig. 1, it can be concluded that the pinning effect exerted by the undissolved vanadium precipitates
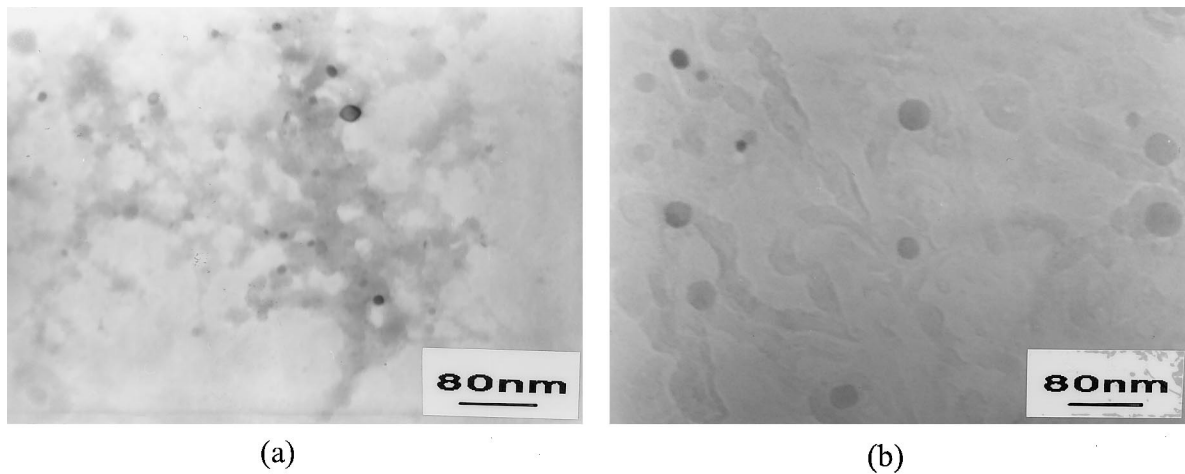
Fig. 10. Precipitation observed in steel V1: (a) as received, (b) after soaking at 870°C.

effect of hot deformation parameters, such as strain, strain rate and temperature, and also some material parameters, such as initial austenite grain size. The impact of the strain can be understood by taking into account that the difference in dislocation density between deformed and undeformed areas constitutes the driving force for recrystallization. Consequently, increasing the strain produces an increment of the dislocation density providing a higher driving force for recrystallization, which translates into a decreasing recrystallization time. A power law dependence of the type $t_{0.5} \propto \varepsilon^{-p}$, with p being a constant taking a value between 2 and 4, is usually found in the literature [12–17]. The effect of strain rate is less than the influence of the other variables but, according to several authors, not insignificant, leading to a decrease on the recrystallization time as the strain rate increases. A typical dependence of $t_{0.5} \propto \dot{\varepsilon}^{-q}$, with q a constant taking different values for different materials, has been reported [13–17]. With respect to material parameters, the effect of the grain size must be considered first. Recrystallized grains nucleate mainly on austenite grain boundaries. When the grain size reduces, the specific grain boundary area increases, providing more sites for nucleation of new grains and, consequently, reducing the time required for recrystallization. A dependence of $t_{0.5} \propto D_{o}^{m}$, is normally observed [12–17]. An exponent $m = 2$ has been often reported in the literature [12]; however, according to other authors, a linear dependence, i.e. $m = 1$, agrees better with experimental data [16,17]. In the present work, the effect of the previous parameters has not been studied directly, and the values of the constants determined for plain carbon and V microalloyed steels, have been taken from the literature as follows [17]: $p = 2$, $q = 0.44$ and $m = 1$. Although in the plane strain compression tests performed in this work a constant strain rate has been used, in order to compare the actual results with other data found in the

bibliography, the influence of strain rate has also been considered.

In microalloyed steels, another factor that can influence the recrystallization kinetics is the solute drag effect exerted by the microalloying elements dissolved in the austenite during reheating. It is well known that the microalloying elements in solution can retard recrystallization, even though they are less effective than if precipitated [18]. In V1 and V2 steels, a higher amount of vanadium is dissolved in the austenite as the reheating temperature increases. Consequently, the 50% recrystallization times determined by Eq. (1) can be affected by the solute concentration of the microalloying element, leading to longer recrystallization times than would have been obtained if solute drag did not occur. In order to differentiate the contribution of this effect, it is necessary to quantify the amount of the microalloying element dissolved at each reheating temperature and also to evaluate how this amount of solute modifies the recrystallization kinetics.

Several experimentally based equations have been proposed in the literature to predict the influence of solutes on static recrystallization kinetics [19,20]. In the case of Nb microalloyed steels, the following expression proposed by Dutta and Sellars [19] is commonly used to quantify the solute effect:

$$t_{0.5} \propto \exp\left[\left(\frac{275\,000}{T} - 185\right)\cdot [C]\right] \tag{5}$$

where $[C]$ is the Nb concentration in solution (wt.%) and T is the deformation temperature. The solute effect of different microalloying elements on static recrystallization was studied by Jonas et al. [6,18]. These authors defined a solute retardation parameter for static recrystallization (SRP), which quantifies the delay produced in recrystallization time by the addition of 0.1% of the different alloy elements to a C–Mn base steel. They found that niobium was the most potent element

in retarding static recrystallization, followed by Ti, Mo and V listed in decreasing order of effectiveness. For niobium, this parameter reached a value of SRP = 222, while in the case of vanadium a notably smaller value of SRP = 13 was calculated. This means that the drag produced by 0.1% V would be equivalent to that made by an amount of 0.005 85% Nb. Taking into account this relationship, Eq. (5) could also be applied to V microal-

loyed steels if the amount of element concentration in solution is modified by the corresponding multiplying factor, thus [C] = 0.0585[V].

In order to compare the recrystallization behavior of the three steels, the differences in initial austenite grain size (D_o), applied strain ($\varepsilon = 0.3$–0.4) and amount of vanadium present in solution at each deformation temperature must be taken into account. For that purpose, once the values of the constants, p, q and m, and the amount of dissolved vanadium are known, a corrected time, denoted as $t_{0.5}^*$, is defined in the following manner:

$$t_{0.5}^* = \frac{t_{0.5}}{\varepsilon^{-2} \dot{\varepsilon}^{-0.44} D_o \cdot \exp\left[\left(\frac{275\,000}{T} - 185\right) \cdot 0.0585 \cdot [V]\right]}$$

(6)

The amount of vanadium present in solution at each reheating temperature, [V], has been calculated from the solubility product equations proposed by Narita for vanadium carbides [21] and by Irvine et al. for vanadium nitrides [22]. The use of $t_{0.5}^*$ allows one to compare data that correspond to different deformation and material parameters. The data of $t_{0.5}$ indicated in Table 2 were corrected by the different contributing factors using Eq. (6) and the resulting values of $t_{0.5}^*$ are presented in Fig. 11 as a function of deformation temperature. From the figure, it can be observed that, while in the case of C–Mn steel there are small changes in $t_{0.5}^*$ with deformation temperature in both microalloyed steels, the corrected time drastically increases as the temperature decreases. It is worth emphasizing that, at 1025°C, the three steels show small differences in behavior. At this temperature, a high amount of vanadium is in solution. At lower temperatures, the retardation of recrystallization time is clearly observed in microalloyed steels in comparison with the C–Mn steel. This behavior is related to the presence of small precipitates that remain undissolved in the austenite during reheating at low temperatures and can exert a retarding effect on recrystallization process.

If, in agreement with Eq. (1), the time $t_{0.5}^*$ is plotted against the inverse absolute temperature on a logarithmic scale (see Fig. 12), the activation energy for recrystallization can be determined from the slopes of the straight lines. From the figure, it can be observed that, in the range of low deformation temperatures, the times required for a 50% recrystallization are significantly higher for the two V microalloyed steels than for the C–Mn steel. At the highest temperature of 1025°C, the times approach each other. The times for the microalloyed steels are slightly longer than that for the C–Mn steel. For the latter steel, a value of $Q = 180$ kJ mol^{-1} was obtained, whereas a higher activation energy, 267 kJ mol^{-1}, was calculated for the microalloyed steels.

In Fig. 13, the present results have been drawn together with additional data previously determined by
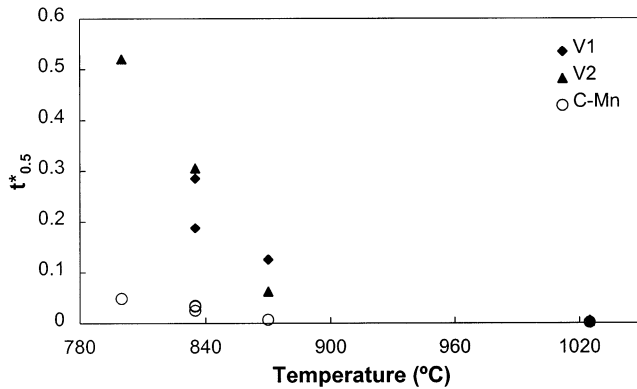

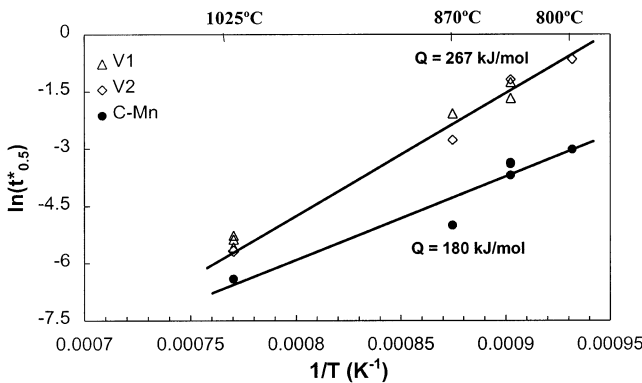Fig. 11. Variation of the corrected time $t_{0.5}^*$ (Eq. (6)) with testing temperature.

Fig. 12. Plot of the empirical relation $t_{0.5}^*$ (Eq. (6)) against the reciprocal of the absolute temperature.
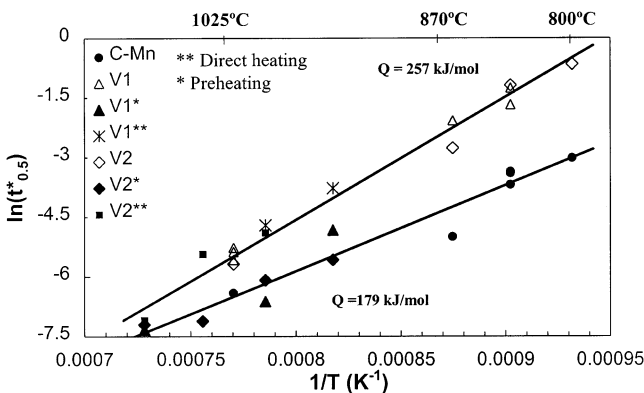

Fig. 13. Plot of the empirical relation $t_{0.5}^*$ (Eq. (6)) against the reciprocal of the absolute temperature. *, **, Data from Ref. [23].

torsion tests on steels V1 and V2 [23]. These tests were carried out under two different conditions: in some cases, the specimens were directly heated to the testing temperature in the range 950–1100°C; other tests were performed with a previous reheating treatment at temperatures of 1100 and 1125°C (30 min), for steel V1 and V2, respectively, to assure a complete dissolution of vanadium precipitates prior to deformation. As can be observed in Fig. 13, all the results of the C–Mn steel and those corresponding to V microalloyed steels at conditions where vanadium precipitates have been completely dissolved before deformation can be ascribed within experimental scatter to the same straight line, denoting that the correction of the solute drag effect of vanadium by Eq. (6) gives reasonable results. From the slope of the straight line, an activation energy of $Q = 179$ kJ mol^{-1} has been calculated in accordance with the value previously obtained for the C–Mn steel in Fig. 12. This value is in good agreement with other data reported in the literature for C–Mn steels [24]. Otherwise, it can be observed that the recrystallization times obtained in specimens directly heated to the deformation temperature follow a different trend. Although in the range of high temperatures both sets of data are close to each other, as the temperature decreases the times observed for direct heating conditions gradually separate from the line followed by the C–Mn steel and the microalloyed steels after previous reheating, leading in the warm working regime to longer $t_{0.5}^{*}$ values than predicted by the previous line. The new set of data can be fitted to another straight line that gives an activation energy of 257 kJ mol^{-1}, very similar to that previously obtained for the present data in the low-temperature range (see Fig. 12).

This significant delay in recrystallization time observed in the warm working regime of the microalloyed V steels differs from the behavior assigned to a solute drag effect or to a strain-induced precipitation. Usually, the interaction between solute drag and static recrystallization shifts the Avrami curve towards longer times, leaving constant the exponent n, as has been described by Jonas et al. for different alloying elements [6,18]. However, as already mentioned, the induced delay in static recrystallization by solute drag in the case of vanadium should be very limited compared with other elements. Similarly, an increase in $t_{0.5}$ due to precipitation during recrystallization is not expected because of the lack of V supersaturation under these conditions. As a consequence, the only main difference in the warm working stems from the presence of undissolved V(C,N) precipitates before the deformation.

In a previous work, Revidriego [23] observed that the no-recrystallization temperature (T_{nr}) determined in multipass torsion tests notably increased in V microalloyed steels when low preheating temperatures, promoting an incomplete dissolution of precipitates, were applied. This author suggested that the undissolved precipitates slow down recrystallization. In the present case, a similar effect can be assigned to the small precipitates in the warm working regime. Nevertheless, the interaction between precipitation and recrystallization is different to that usually observed in hot working. In the latter case, below the non-recrystallization temperature, strain-induced precipitation takes place during recrystallization, modifying the kinetics and, in some cases, stopping it. When it takes place, the recrystallization curves show a plateau after a certain time, which is taken as the precipitation start time [25,26]. However, in warm working, the precipitates are present prior to the onset of recrystallization and, according to the results obtained in the present study, they retard the recrystallization process as a whole. As a consequence of this, the kinetics is slowed down and Avrami equation presents a lower value of the exponent n.

From Figs. 11 and 12, it is clearly evident that the delay is more significant, in comparison with the C–Mn steel, in the range of low deformation temperatures. To take into account this effect, the size and volume fraction of precipitates have to be analyzed at 835 and 870°C. The interaction between precipitation and recrystallization can be considered in terms of the driving forces related to both mechanisms [5,7,27]. The driving force for recrystallization can be estimated from [27]:

$$F_{rex} = 12.5(\Delta\sigma)^2 \mu^{-1} \tag{7}$$

where μ is the temperature-dependent shear modulus [28], and $\Delta\sigma$ is the increase in flow stress during work hardening. Similarly, for the estimation of the precipitation pinning force, the equation corresponding to the flexible boundary model can be considered [7]:

$$F_{pin} = \frac{3\gamma f_v^{2/3}}{\pi r} \tag{8}$$

where f_v is the precipitate volume fraction, r the particle radius and γ the interfacial energy per unit area of boundary, taken as 0.8 J m^{-2} [7,27]. When $F_{pin} > F_{rex}$, recrystallization should be completely arrested [5].

The recrystallization and precipitation forces have been calculated at 835 and 870°C for both microalloyed steels, and the resulting values are listed in Table 3. The pinning forces were calculated using the mean precipitate size value measured for each reheating temperature, and the volume fraction determined from the relationship with the number of precipitates per unit area [29] (see Table 3). From the data of the table, the pinning forces exerted by the precipitates are always smaller than F_{rex}, confirming that the present V(C,N) precipitates are not sufficient to stop recrystallization. Nevertheless, comparing the values of the pinning forces at 870 and 835°C, it results that there is a significant increase in the latter case. This change, due mainly to the presence of a higher fraction of undis-

Table 3
Estimated recrystallization and pinning forces at 870 and 835°C ($\varepsilon = 0.3$, $\dot{\varepsilon} = 10$ s^{-1})

Temperature (°C)	Steel	$\Delta\sigma$ (MN/m^2)	f_v (%)	F_{rex} (MN/m^2)	F_{pin} (MN/m^2)
	V1	168	0.0031	7.5	1.7
870	V2	150	0.0034	6.0	1.6
	C–Mn	137	–	5.1	–
835	V1	178	0.0068	8.2	4.8
	V2	191	0.0081	9.5	3.4
	C–Mn	146	–	5.6	–

solved precipitates when lower reheating temperatures are considered, can explain at least qualitatively the observed retardation in the recrystallization measured at 835°C with respect to that at 870°C. Although precipitation measurements have not been carried out at 800°C for steel V2, a similar behavior should be expected to be responsible for the greater delay at this temperature.

It is worth emphasizing that, in both V microalloyed steels, the effect of the precipitates can be assigned to the group defined by Hansen et al. [5] as $F_{rex} > F_{pin}$, in which grain boundary migration could take place but at some reduced overall velocity. Consequently, recrystallization can be retarded but not completely stopped as it occurs when strain-induced precipitation occurs during recrystallization, in which case F_{pin} is larger than F_{rex} [27]. From Fig. 13, it can be seen that the retardation on recrystallization produced by the precipitates present before deformation extend to higher temperatures. However, as expected, its effect gradually decreases as the temperature increases because of the reduction in the number of precipitates that can pin the grain boundaries, due to both their increased dissolution and coarsening.

Another aspect that must be taken into account is that the delay in recrystallization is observed during the overall period in which it takes place, as can be deduced from the Avrami curves. Due to the lack of supersaturated vanadium in the austenite, the precipitate growth process will be notably slower than that corresponding to hot working conditions with high soaking temperatures and, in consequence, significant supersaturation levels. In these latter cases, the growth of precipitates leads to a loss of their pinning effect after some limited time. This behavior has also been observed in V microalloyed steels in the temperature range 800–850°C (with a previous soaking at 1200°C and complete dissolution of precipitates), where a significant precipitate growth is measured during the period in which recrystallization is delayed [30]. In contrast, for the testing temperatures analyzed in this work, in agreement with the results of Rivas et al. [31], it can be assumed that a small particle coarsening will take place during the time required for recrystallization completion.

5. Conclusions

For vanadium microalloyed steels, a retardation on static recrystallization is observed as compared with plain carbon steel. The origin of this delay depends on the testing temperature.

At high temperatures, in the range of full static recrystallization during hot working, a small delay is observed that is attributed to the solute drag effect of vanadium.

At lower temperatures, corresponding to warm working conditions, an increased delay is observed as the temperature decreases due to the presence of undissolved small precipitates that have a retarding effect on the recrystallization kinetics. The interaction between precipitates and recrystallization is different to that observed for hot working conditions where strain-induced precipitation takes place during recrystallization. In warm working, the precipitates are already present before deformation and retard the recrystallization process as a whole, resulting in a lower value of the Avrami exponent and higher $t_{0.5}$ times.

References

[1] M. Korchynsky, J.R. Paules, SAE Technical Paper number 890801, 1989.
[2] S. Engineer, B. Huchtemann, in: C.J. Van Tyne, G. Krauss, D.K. Matlock (Eds.), Fundamentals and Applications of Microalloying Forging Steels, TMS, Warrendale, PA, 1996, pp. 61–78.
[3] C. Garcia-Mateo, J.L. Romero, J.M. Rodriguez-Ibabe, Proceedings of the 41st Mechanical Working and Steel Processing Conference, vol. 37, Warrendale, PA, USA, 1999, pp. 653–663.
[4] C. Garcia-Mateo, J.L. Romero, J.M. Rodriguez-Ibabe, Mater. Sci. Forum 284–286 (1998) 435–442.
[5] S.S. Hansen, J.B. Vander Sande, M. Cohen, Metall. Trans. 11A (1980) 387–402.
[6] H.L. Andrade, M.G. Akben, J.J. Jonas, Metall. Trans. 14A (1983) 1967–1977.

[7] O. Kwon, A.J. DeArdo, Acta Mater. 39 (1991) 529–538.

[8] W.J. Liu, J.J. Jonas, Metall. Trans. 19A (1988) 1403–1413.

[9] L.P. Karjalainen, Mater. Sci. Technol. 11 (1995) 557–565.

[10] G.J. Richardson, D.N. Hawkins, C.M. Sellars, Worked Examples in Metal Working, The Institute of Metals, London, 1985.

[11] P.T. Mazzare, S.W. Thompson, G. Krauss, in: A.J. DeArdo (Ed.), Proceedings of the International Conference on Processing, Microstructure and Properties of Microalloyed and Other Modern HSLA Steels, ISS, Warrendale, PA, 1992, pp. 497–509.

[12] C.M.Sellars, in: C.M. Sellars, G.J. Davies (Eds.), Proceedings of the International Conference on Hot Working and Forming Processes, Metals Society, London, 1980, pp. 3–15.

[13] K. Airaksinen, L.P. Karjalainen, D. Porter, J. Perttula, in: J.M.Rodríguez-Ibabe et al. (Eds), Proceedings of the International Conference on Microalloying in Steels, μ-as, S. Sebastian, Trans Tech Publications, Switzerland, 1998, pp. 119–126

[14] L.P. Karjalainen, J.S. Perttula, in: T.R. McNelly (Ed.), Proceedings of the 3rd International Conference on Recrystallization and Related Phenomena, Rex'96, Monterrey, MIAS, Monterrey, 1996, pp. 413–420.

[15] W.P. Sun, E.B. Hawbolt, ISIJ Int. 37 (1997) 1000–1009.

[16] S.F. Medina, J.E. Mancilla, ISIJ Int. 36 (1996) 1070–1076.

[17] S.F. Medina, J.E. Mancilla, C.A. Hernandez, ISIJ Int. 34 (1994) 689–696.

[18] J.J. Jonas, in: D.P. Dunne, T. Chandra (Eds.), High Strength Low Alloy Steels, Wollongong, Australia, 1984, pp. 80–91.

[19] B. Dutta, C.M. Sellars, Mater. Sci. Technol. 3 (1987) 197–206.

[20] C.M. Sellars, J.H. Beynon, in: D.P. Dunne, T. Chandra (Eds.), High Strength Low Alloy Steels, Wollongong, Australia, 1984, pp. 142–150.

[21] K. Narita, Trans. ISIJ 15 (1975) 145–152.

[22] K.J. Irvine, F.B. Pickering, T. Gladman, JISI 205 (1967) 161–182.

[23] F.J. Revidriego, Master Thesis, University of Navarra, 1995.

[24] S.F. Medina, J.E. Mancilla, ISIJ Int. 36 (1996) 1063–1069.

[25] S.F. Medina, J.E. Mancilla, Acta Metall. Mater. 42 (1994) 3945–3951.

[26] P. Uranga, A.I. Fernández, B. López, J.M. Rodriguez Ibabe, Thermomechanical Processing of Steels 1 (2000) pp. 204–213.

[27] E.J. Palmiere, C.I. Garcia, A.J. DeArdo, Met. Trans. 27A (1996) 951–960.

[28] H.J. Frost, M.F. Ashby, Deformation Mechanisms Maps, Pergamon Press, Oxford, 1982.

[29] M.F. Ashby, E. Ebeling, Trans. AIME 236 (1966) 1396–1404.

[30] A.B. Quispe, S.F. Medina, J.M. Cabrera, J.M. Prado, Mater. Sci. Technol. 15 (1999) 635–642.

[31] A.L. Rivas, D.M. Michal, M.E. Burnett, C.F. Musolff, in: C.J. Van Tyne, G. Krauss, D.K. Matlock (Eds.), Fundamentals and Applications of Microalloying Forging Steels, TMS, Warrendale, PA, 1996, pp. 159–172.